ENCIT 2018

ABCM Associação Brasileira de Engenharia e Ciências Mecânicas

17th Brazilian Congress of Thermal Sciences and Engineering
November 25th-28th, 2018, Águas de Lindóia, SP, Brazil

ENCIT-2018-0200
THE USE OF MEASURED DATA IN THE PREDICTION OF A DEVELOPED SLUG FLOW PATTERN FOR CFD SIMULATIONS

Matheus Martinez Garcia
Marcelo Souza de Castro
University of Campinas, Campinas, Brazil
m147395@dac.unicamp.br, mcastro@fem.unicamp.br

Abstract. *A method for the minimization of the computational cost spent during the development of a slug flow pattern in CFD simulations is proposed. The method is based on setting a prediction of the flow variables, e.g. phases' distribution, velocity field, and so forth in the inlet of the domain. The imposed slug flow is obtained using the measured data of other simulations or experiments, along with mechanistic models found in literature. The CFD simulations were carried out in OpenFOAM using RANS equations, with the standard k-ϵ model being used for the turbulence modelling. The approach suggested and tested during this text was capable of generating small Taylor bubbles, but the result isn't ideal. Possible approaches to deal with the problems found in the simulations are described in the Future Works Section, and the final results are going to be published in the congress poster.*

Keywords: *CFD, slug flow, computational cost, simulation, prediction*

1. INTRODUCTION

An important feature of multiphase flows is the occurrence of several unique flow patterns, which depend on the number of phases, the quantity of each fluid flowing inside the domain, the pipe's geometry, the properties of the fluids, and so forth.

The slug flow is a pattern that may take place in gas-liquid systems and appears in many different industrial applications. The pattern is characterized by the quasi-periodic occurrence of a large bullet-shaped bubble, the Taylor bubble, followed by a liquid slug. The presence of this two distinct zones affects directly the pressure distribution over the flow, due the fact that the Taylor Bubble zone has a small pressure drop, while the liquid slug zone, which has much less gas, is the main responsible for the pressure drop over in the flow. Another characteristic of slug flows is the growth of the bubble in the direction of the flow, because of the pressure drop (decompression).

The gas dominant - liquid dominant transition is marked by a momentum jump in the flow, due the high difference in the density of the fluids. This momentum jump, along with the incompressible characteristic of the liquid phase, may lead to huge impacts (fluid hammer) in the systems where the slug flow takes place. Therefore, it is fundamental to verify the effects of the slug flow in the equipments where it may occur.

The main difficult found when performing a slug flow simulation consists in its computational cost. The intrinsic intermittent characteristic of the pattern, along with the development length required for the formation of the large bubbles are the main barriers for a quick slug flow simulation. Besides that, the complex turbulent structures that take place in the liquid phase during the passage of the bubble almost always limit the numerical approach to a modelled turbulence (RANS).

The focus of this project is to reduce the size of the domain used for the development of a slug flow simulation, in order to reduce its computational cost based on the reduction of the number of elements present in the domain. The method chose to accomplish this is to set the inlet of the simulations with a approximation of the bubble, aiming at reducing the pattern's development length. The choice of setting a boundary condition (at the pipe's inlet) instead of a initial condition (inside the domain) is the capability of generating a continuous slug flow, that can be used for the simulation of industrial components, or to study trails of bubbles.

2. LITERATURE REVIEW

(Abdulkadir *et al.*, 2015) made CFD simulations and experiments regarding gas-liquid slug flows in vertical systems. The authors chose a air-silicone oil mixture for their studies, with the properties described in Tab. 1. The superficial velocities adopted by the authors were V_{sl}=0.05 m/s and V_{sg}=0.344 m/s, at the pipe inlet. A 6m length pipe was used for both the simulations and experiments, with an internal diameter of 67mm.

The authors used a Butterfly (O-grid) mesh with 500,000 cells for their simulations. Both fluids were considered

Table 1: Properties of the fluids used in Abdulkadir *et al.* (2015)

Property	Air	Silicone Oil
Density	1.18 kg/m^3	900 kg/m^3
Viscosity	18e-6 Pa.s	5.3e-3 Pa.s
Surface Tension	0.02 N/m	

incompressible and the standard k-ϵ was used for the turbulence modelling. They used the Star-CCM+ to perform the numerical approach, attaining good results in comparison to the obtained experimental data.

(Tocci, 2016) replicated the case studied by (Abdulkadir *et al.*, 2015), but using the OpenFOAM instead of the Star-CCM+ to perform the simulations. The author stated that the pure VoF approach, represented inside the OpenFOAM by the solver `interFoam`, is not sufficient to properly represent the slug flow that should take place under the imposed conditions of (Abdulkadir *et al.*, 2015). Moreover, (Tocci, 2016) states that a euler-euler approach should be used for the flow simulation, represented in the OpenFOAM by the solver `multiphaseEulerFoam`.

The `multiphaseEulerFoam` was developed by (Wardle and Weller, 2013). The solver was developed with the mind-set of solving the major structures of the flow, while modelling the minor structures, composed by the dispersed phase. According to (Wardle and Weller, 2013), the pure VoF approach should be used along with a mesh approximately 10 times smaller than the smallest fluid droplet/bubble, in order to achieve an adequate result. This requirement of several elements per bubble usually leads to a huge mesh, with the requirement of very low time steps (because of the solution's stability criteria - based on CFL), which is unaffordable for the most of the scenarios.

The slug flow pattern has an interesting feature regarding its formation, which leads to different approaches depending on the pipe's inclination. For horizontal ducts, the slug flow starts when a interfacial wave touches the pipe ceil (Taitel and Dukler, 1976). The pattern presents small bubbles in the flow, specially in the tail of large bubbles, but the process that causes the transition between stratified flow and slug flow depends only on the movement of a well-defined interface. Therefore, the pure VoF approach is able to generate a horizontal slug flow, as made by (Shuard *et al.*, 2016), using the `interFoam`.

The vertical slug flow, on the other hand, is formed due the coalescence of several small bubbles present in the flow (Taitel *et al.*, 1980). Therefore, in a CFD simulation, it would be necessary to represent the movement of the small bubbles in order to reproduce this mechanism, leading to the problem reported by (Wardle and Weller, 2013), about the necessity of many elements inside the computational domain. As consequence, the use of the solver `interFoam` doesn't lead to satisfactory results, and a model representing the dispersed phase should be used in a scenario where solving the dispersed phase isn't affordable. In OpenFOAM, several models for the dispersed phase can be used along with the solver `multiphaseEulerFoam`, regarding the virtual mass of these bubbles, the drag caused by their presence, among others.

3. NUMERICAL METHODS

3.1 MESH

The butterfly mesh was adopted for the simulations, based on the previous works of (Hernandez-Perez *et al.*, 2011; Abdulkadir *et al.*, 2015; Tocci, 2016). The domain and properties are the same reported by (Abdulkadir *et al.*, 2015; Tocci, 2016), consisting in a 6m-long pipe, with the internal diameter of 67mm, and the fluid properties described in Tab. 1. The butterfly mesh is marked by the presence of two distinct zones: a cylindrical grid close to the wall, and a cartesian grid in the middle of the tube. The Cross-section of the mesh used in this work is shown in Fig. 1.

The mesh of Fig. 1 has 448 elements in each cross-section, and 1080 equally-distributed cells in the axial direction. This distribution of elements results in a mesh of almost 500,000 elements, which is the value adopted by (Abdulkadir *et al.*, 2015). The first elements in contact were designed to ensure $y^+ < 5$ for the expected velocities, in order to properly represent the turbulent effects.

(Tocci, 2016) repeated the same case of study of (Abdulkadir *et al.*, 2015), but using a mesh with the double number of elements, around a million, and using the OpenFOAM for the simulations. It will be seen in the Results' section that the number of elements adopted by (Abdulkadir *et al.*, 2015) was enough to properly represent the flow, even when using the OpenFOAM.

3.2 HYPOTHESIS AND EQUATIONS

The `multiphaseEulerFoam` was developed to solve a system of n incompressible and isothermal phases. Therefore, the mass balance of each phase, j, is given, in the differential form, by Eq. 1.

$$\frac{\partial \alpha_j}{\partial t} + \nabla \cdot (\overrightarrow{u_j} \alpha_j) = 0 \tag{1}$$

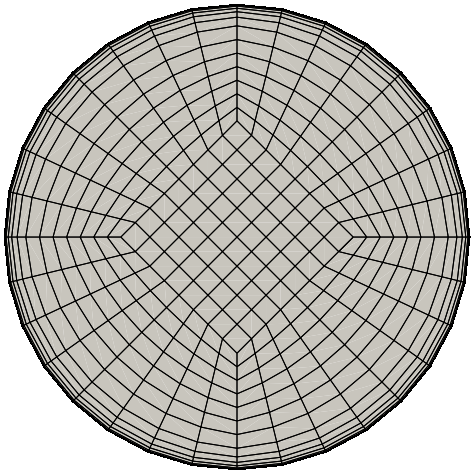

Figure 1: Mesh of a cross-section of the tube.

In Eq. 1, α_j is a phase-tracking function, with a comportment analogous to the void fraction of each mesh's cell. Therefore, it has a value between 0 and 1, and the sum of α_j should be 1 for each cell in the domain.

The momentum equation for the j-phase is given by Eq. 2. In this equation, $\overrightarrow{f_{d,j}}$ represents the drag force (per unity of volume) acting on the phase j, and the $\overrightarrow{f_{s,j}}$ represents the surface tension forces acting on the same phase.

$$\frac{\partial\left(\rho_j\alpha_j\overrightarrow{u_j}\right)}{\partial t}+\nabla\cdot\left(\rho_j\alpha_j\overrightarrow{u_j}\overrightarrow{u_j}\right)=-\alpha_j\nabla p+\nabla\cdot\left(\mu_j\alpha_j\nabla\overrightarrow{u_j}\right)+\rho_j\alpha_j\overrightarrow{g}+\overrightarrow{f_{d,j}}+\overrightarrow{f_{s,j}} \tag{2}$$

The surface tension force is based on the Continuum Surface Force (CSF) model developed by (Brackbill *et al.*, 1992). The drag therm is modelled as Eq. 3. In Eq. 3, the subscript "c" represents the continuum phase and the subscript "d" represents the dispersed phase. The simulations of this report were made considering that both phases can have dispersed elements (blended type in OpenFOAM).

$$\overrightarrow{f_{d,j}}=\alpha_c\alpha_d K\left(\overrightarrow{u_d}-\overrightarrow{u_c}\right) \tag{3}$$

In `multiphaseEulerFoam`, several drag models are available for choice. The drag model used in this text was developed by (Schiller and Naumann, 1935). The model is summarized in Eqs. 4, 5 and 6, taken from (Weller, 2008). This was the same model used by (Tocci, 2016).

$$K=\frac{3}{4}\rho_c C_d\frac{|\overrightarrow{u_d}-\overrightarrow{u_c}|}{d_d} \tag{4}$$

$$C_d=\begin{cases}\frac{24\left(1+0.15Re^{0.683}\right)}{Re}, & \text{if } Re\leq 1000\\ 0.44, & \text{if } Re>1000\end{cases} \tag{5}$$

$$Re=\frac{|\overrightarrow{u_d}-\overrightarrow{u_c}|d_d}{\nu_c} \tag{6}$$

The solver (in the OF-16.12+ version) allows two options for the dispersed phase diameters. The constant diameter approach and the isothermal approach. This project adopts the constant diameter of 0.1mm for the silicone droplets and the isothermal diameter model for the gas phase, with the diameter of 3mm at atmospheric pressure used for reference. The isothermal model corrects the dispersed-phase diameter considering the ideal gas law, with the assumption of isothermal flow.

Eq. 1 is modified during the implementation of the solver to add the interface compression term developed by (Weller, 2008), leading to Eq. 7. Note that the new term acts only in mixture cells (where $0\leq\alpha\leq 1$).

$$\frac{\partial \alpha_j}{\partial t} + \nabla \cdot (\overrightarrow{u_j}\alpha_j) + \nabla \cdot [\alpha_j (1 - \alpha_j) \overrightarrow{u_s}] = 0 \tag{7}$$

The compression velocity, $\overrightarrow{u_s}$, is given by Eq. 8, where C_α has a value between 0 and 1. In this text, as in (Tocci, 2016), $C_\alpha = 1$

$$\overrightarrow{u_s} = C_\alpha |\overrightarrow{u}| \frac{\nabla \alpha}{|\nabla \alpha|} \tag{8}$$

The `multiphaseEulerFoam` solver uses a homogeneous model for turbulence (shared by both phases). The standard k-ϵ, proposed by (Launder and Spalding, 1983), was used for the turbulence modelling during the simulations of this report, as made by (Abdulkadir *et al.*, 2015; Tocci, 2016). (Launder and Spalding, 1983) also proposed some equations for the inlet values of the turbulent parameters, represented in Eqs. 9, 10 and 11.

$$k_{in} = \frac{3}{2} (UI)^2 \tag{9}$$

$$\epsilon_{in} = 2 \frac{k_{in}^{3/2}}{D} \tag{10}$$

$$I = \frac{0.16}{Re^{1/8}} \tag{11}$$

3.3 INITIAL AND BOUNDARY CONDITIONS

3.3.1 BOUNDARY CONDITIONS

The boundary conditions adopted in this text are summarized in Tab. 2, for every field (both scalar and vectorial) used by the `multiphaseEulerFoam` solver. The numbered BCs of Tab. 2 aren't fixed. They depend on the method of fluid injection, always representing the values of the fields at their respective boundary surfaces. The numbered BCs are going to be explored in Section 3.5 It is important to emphasise that the "fixedFluxPressure" condition is fundamental to the appearance of the slug flow in the simulation, according to the tests realized during this project.

Table 2: Boundary conditions adopted for the simulations.

Field	Inlet	Outlet	Wall
alpha.air	Dirichlet condition[1]	inletOutlet, inletValue=1	zeroGradient
alpha.silicone	Dirichlet condition[1]	inletOutlet, inletValue=0	zeroGradient
alphas	calculated	calculated	calculated
U.air	Dirichlet condition[2]	pressureInletOutletVelocity	fixedValue (0 0 0)
U.silicone	Dirichlet condition[2]	pressureInletOutletVelocity	fixedValue (0 0 0)
p_rgh	fixedFluxPressure	totalPressure uniform 154,299	zeroGradient
p	calculated	calculated	calculated
k	Dirichlet condition[3]	zeroGradient	zeroGradient
epsilon	Dirichlet condition[3]	zeroGradient	epsilonWallFunction
nut	calculated	calculated	nutUWallFunction

3.3.2 INITIAL CONDITIONS

The initial condition was adopted as the tube filled with static liquid. Therefore, alpha.air=0, alpha.silicone=1 and U.air=U.silicone=(0 0 0). The pressure used by the solver is the modified pressure, p_rgh, which consists in the static pressure plus the "hydrostatic" component ($\rho_j g h$). Therefore, the p_rgh scalar field was considered with a uniform value of 154,299Pa, which leads to the atmospheric pressure at the outlet, if the liquid phase is considered at this location.

The k and epsilon initial values were adopted according to Eqs. 9, 10, 11. It should be noted that these values lead to a hydrodynamic instability (Rayleigh-Taylor) in the first time steps of the simulation. (Abdulkadir *et al.*, 2015; Tocci, 2016) adopted different values of k and ϵ to avoid this instability. As consequence, the first bubble obtained during the simulations of this project don't have the same shape obtained by the authors, because of the residual effects of the initial conditions adopted. However, for the rest of the flow, the results obtained in the project share the same characteristics of the results obtained by the other authors.

3.4 SOLVER SETTINGS

Second-order centered schemes with flux limiters were adopted for the spatial discretization (Van Leer Schemes).The implicit euler method was adopted for the time discretization. The time step was set to 5e-5s, ensuring $CFL < 0.2$.

3.5 INLET CONDITIONS

Two distinct sets of inlet conditions were considered during this project, until this report. The first one consisted in replicating the same BCs used by (Abdulkadir *et al.*, 2015), in order to compare the results obtained with the results obtained by the author. The second set of inlet conditions was developed to inject a measured slug flow into the domain.

3.5.1 VALIDATION OF THE MODEL

The validation method consists in replicating the study of Abdulkadir *et al.* (2015). The authors adopted the use of the homogeneous model ((Wallis, 1969)) to set the inlet conditions. Considering $V_{sl} = 0.05$ m/s and $V_{sg} = 0.344$ m/s, the velocity at inlet is given by $V_m = V_{sl} + V_{sg} = 0.394$ m/s. The no-slip hold up ratio is given by the ratio between the superficial velocity and the mixture velocity, for each phase. Therefore, $\alpha \approx 0.13$, and the numbered items of Tab. 2 are as follows: 1- fixedValue, with the values of uniform 0.13 for the silicone oil and uniform 0.87 for the air; 2- fixedValue uniform 0.394 for both phases; 3- fixedValue, given by Eqs. 9 and 10 for their respective variables, and using the mixture's properties to estimate the Reynolds number in Eq. 11.

To compare the results with the literature, the data was acquired using an integral filter, which integrates the void fraction (alpha.air) over the surface for some cross-sections of the tube. The cross-sections chosen for the analysis of the results are: z=0.5m, z=1.0m, z=1.5m, z=2.0m, z=2.5m, z=3.0m, z=4.0m, z=4.4m, z=4.489m, z=4.5m and z=5.0m. The interval of measurement was set to 0.01s.

3.5.2 MIXTURE REINJECTION

The approach used for the mixture reinjection consists in measuring the space-average of the void fraction at a determined cross-section of the tube as a function of time, and using this data as the inlet boundary condition. The measured section adopted was located at $z = 4m$, where, as reported by (Abdulkadir *et al.*, 2015; Tocci, 2016) and by the validation herein realized, the slug flow was fully developed.

The measured data was converted to a table, and reinserted at the inlet using the "uniformFixedValue" BC. This function reads the table and uses a linear interpolation between the intervals of the measured data to set uniform values (in the inlet section) of the read variables.

Two different files were built, one for the alpha.air and one for the alpha.silicone, and the inlet condition of Tab. 2 becomes "uniformFixedValue" for both fields, each one reading its own data. The other numbered conditions (2 and 3) are kept the same as in the validation scenario.

4. RESULTS AND DISCUSSION

4.1 MODEL VALIDATION

4.1.1 Taylor Bubble Occurrence

(Abdulkadir *et al.*, 2015) adopts the idea of (Costigan and Whalley, 1997) of using of the Probability density function (PDF) to characterize the slug flow. In the PDF, the slug flow is characterized by the presence of two peaks on its probability distribution, one for high void fractions and one for low void fractions, representing the occurrence of Taylor Bubbles and Liquid Slugs, respectively.

The interval chosen for the PDF analysis ranges between 9.3 and 12.4s. The results obtained are summarized for each section in Tab. 3.

Table 3: Results obtained as function of position.

Position	α as Function of Time	PDF of α

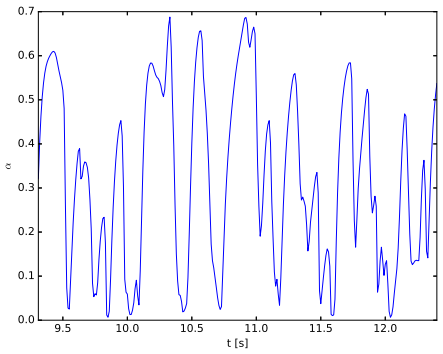

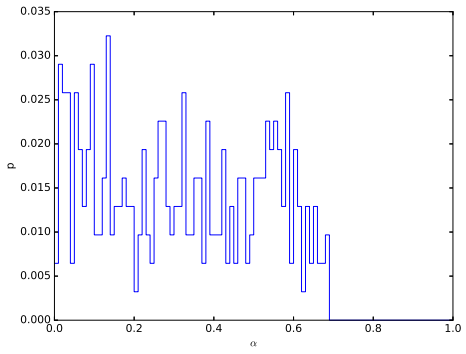

z=0.5m

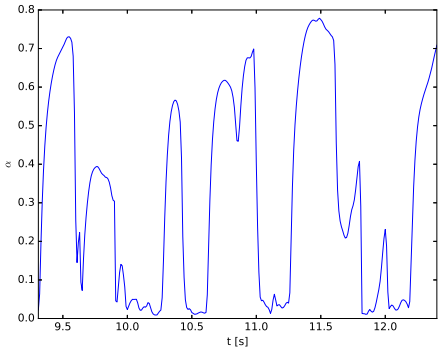

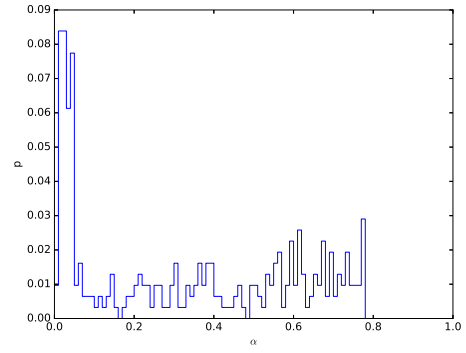

z=1.0m

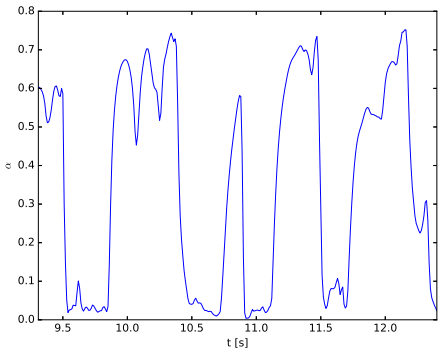

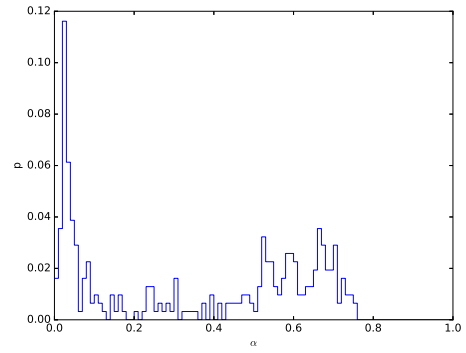

z=1.5m

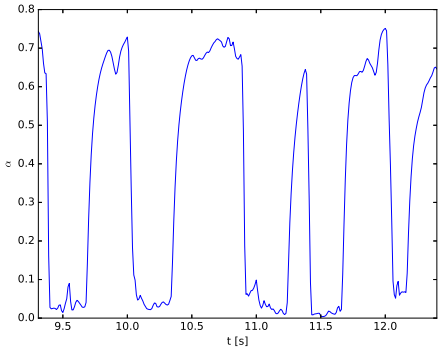

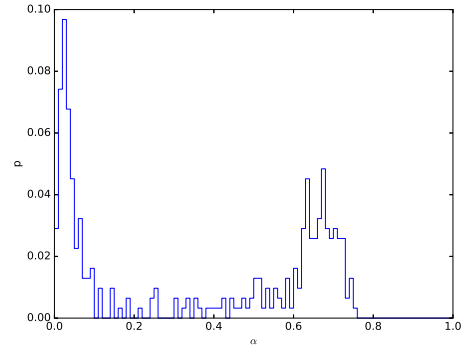

z=2.0m

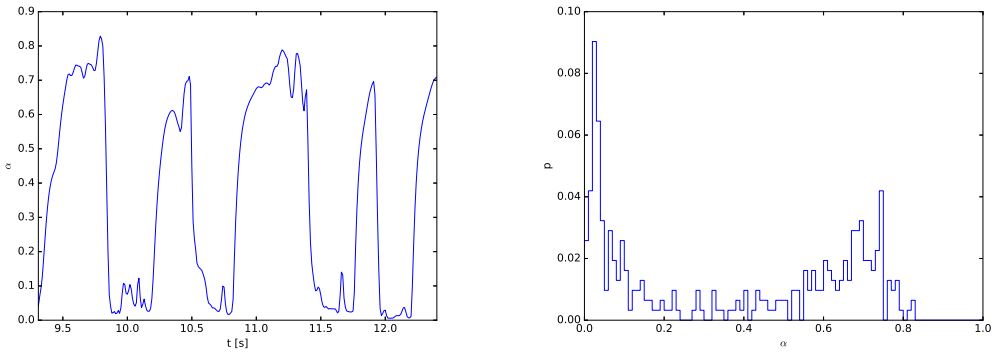

z=2.5m

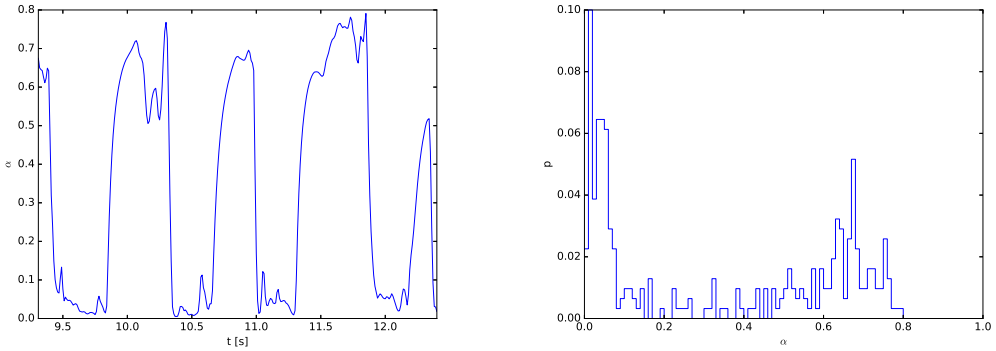

z=3.0m

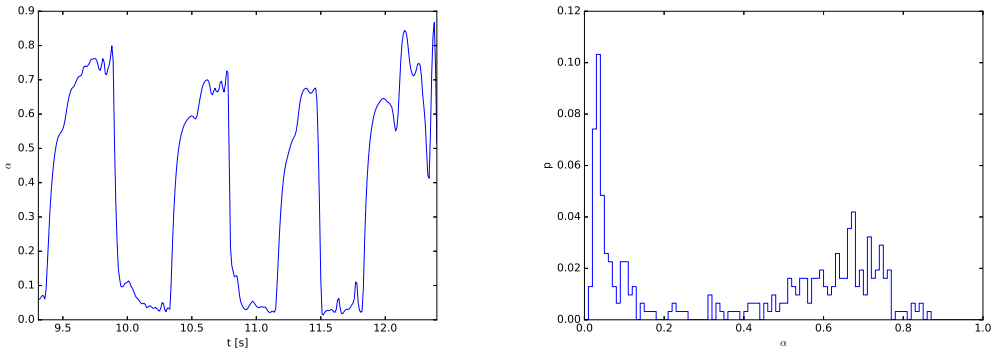

z=3.5m

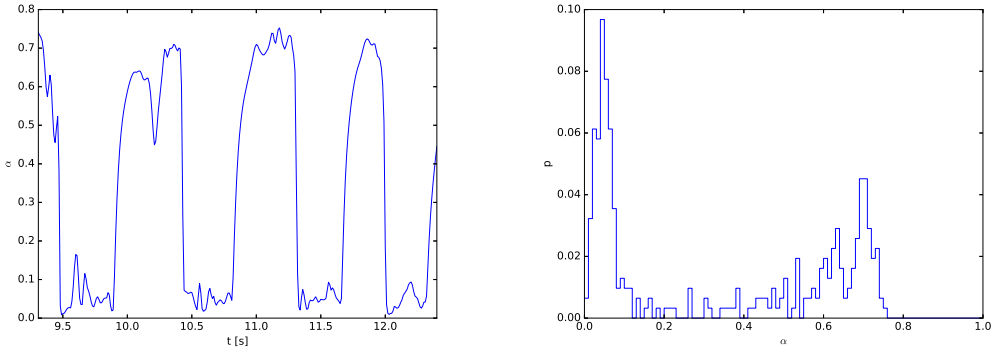

z=4.0m

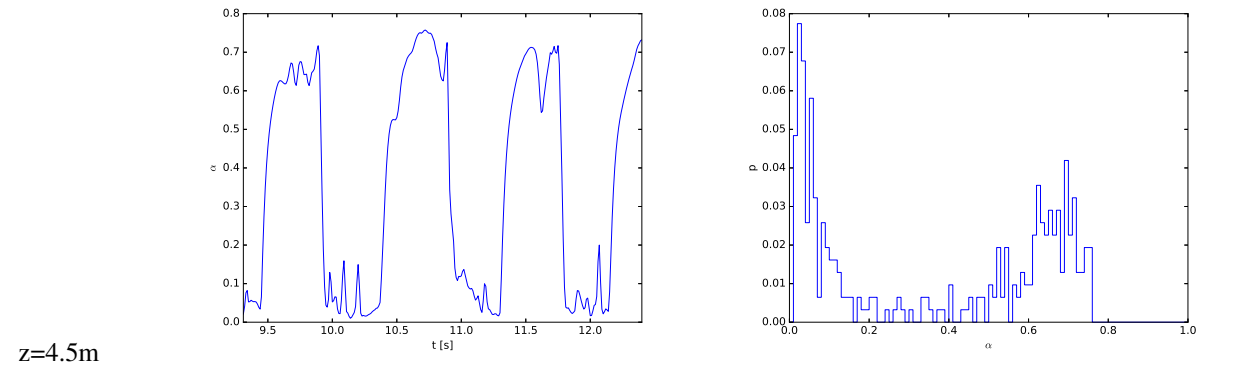

z=4.5m

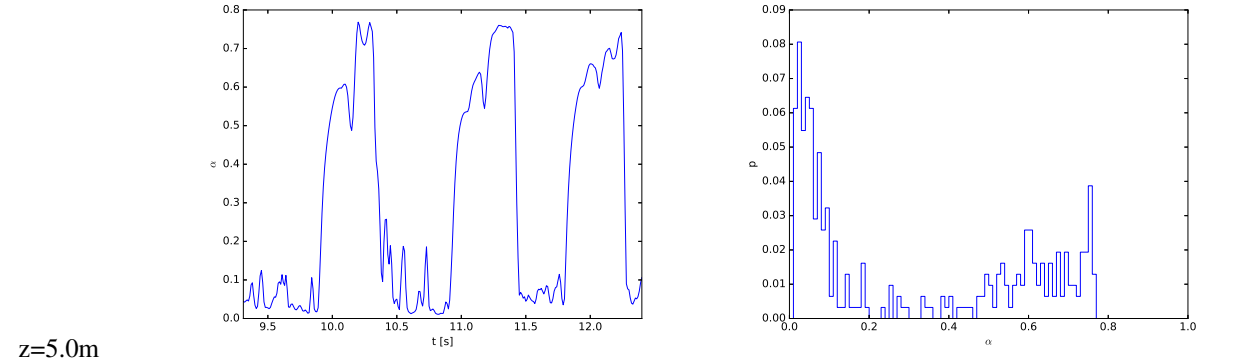

z=5.0m

Table 3 shows that the presence of two peaks in the PDF clearly occurs for $z > 1.5$m. Considering every graph present in Tab. 3, it is possible to identify the absence of intermediary values of α. This result differs from the graphs presented in (Abdulkadir *et al.*, 2015), where intermediary values of alpha were achieved. Besides that, the peaks shown in Tab. 3 are much more evident than in (Abdulkadir *et al.*, 2015). However, the obtained graphs approach the results obtained by (Tocci, 2016), which are closer to the experimental data than the results obtained by (Abdulkadir *et al.*, 2015).

The difference between the results obtained by both authors can be explained by the interface compression factor, C_α. This factor forces the small elements of the flow (the dispersed phase) to agglutinate in bigger elements, avoiding intermediate values of void fraction. The simulations' results are only compatible because of the structure of the slug flow pattern, marked by the presence of big bubbles and low-aerated liquid zones. Thus, after long distances, the results converge to the same answer. This is an indicative that, for highly-aerated liquid slugs the answer probably wouldn't be the same, and a study of this coefficient should be performed in order to allow the formation of cells with intermediate values of void fraction. Besides that, the study of the dispersed phase diameter in the solver response is also important, if this property is not known previously, as in the simulations herein reported.

The αxt curves of Tab. 3 show an interesting feature: the growth and separation of the flow structures. The first meter of the tube present a high-frequency oscillation of the void fraction, indicating that small structures are intercalating at the measured locations. This means that small bubbles are passing through this sections. With the increase in the distance, bigger structures start appearing. The agglutination between two consecutive bubbles reduces 2 slug unities into one. Therefore, by the conservation of mass, the length of the slug unities increase with the distance from the inlet, as more bubbles are joining the major Taylor bubbles. The consequence of this effect is a reduction in the frequency of the αxt curve with the increase in the position, as seen in the curves for the first meters.

At the same time, the density difference between the phases start playing an important role with the increase in the size of the bubbles, because of an unbalance between the viscous effects, that tend to hold the bubble, and the buoyant effects, that cause the bubbles to rise. This phenomena causes the Taylor bubbles that take place during the process of agglutination to be transported faster than the liquid slugs, which also impacts the frequency of the flow.

4.1.2 Taylor Bubble Velocity

After some entrance length, around 3.5m to 4m, the frequency of the curves start converging to an almost-constant value, indicating that the bubbles are moving with the same velocity, V_{tb}. (Abdulkadir *et al.*, 2015) uses the Pearson correlation coefficient to obtain the time delay between the passage of the flow between two different cross-sections of the pipe. The author chose the values of z=4.4m and 4.489m to obtain the α signals. The values of α as function of time

obtained in this work for these sections are presented in Fig. 2

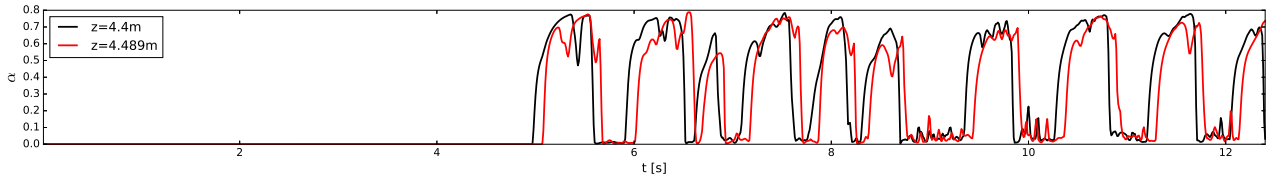

Figure 2: α as function of time for z=4.4m and z=4.489m.

The method used by the author consists in translating one of the signals in time, using different values for the translation. Then, for each time translation, the correlation between the void fractions, for the same time instant (considering the translation in one of the signals) is calculated. A correlation coefficient near to 1 is expected when the time translation is sufficient to overlap both of the signals. The correlation coefficient as function of time delay (time translation) is present in Fig. 3.

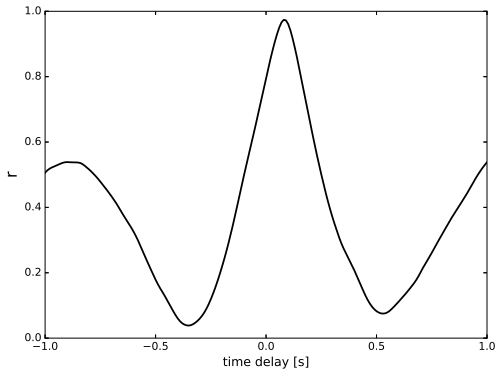

Figure 3: Correlation coefficient as function of the time delay.

The peak of r is obtained at a time delay of 0.08s. This is the same result obtained by (Tocci, 2016), but using half of the mesh elements adopted by the author. The velocity of a Taylor bubble is given by $V_{tb} = (4.489 - 4.4)/0.08 = 1.11m/s$. This indicates that a proper slug flow pattern was developed using the methodology proposed in this text.

4.2 FLUID INJECTION

The result obtained using the injection method proposed is far from the desired. The method was capable of generating small Taylor bubbles, with sizes much smaller than the expected. The liquid slugs formed using the method are also long enough to prevent the reunion of two consecutive bubbles, and the pattern remains composed by little structures indefinitely. The biggest hypothesis for this comportment is the absence of a velocity profile approximation. Because of the buoyant effects, the Taylor bubble moves with a higher speed than the liquid film around it. Sometimes, in order to ensure mass conservation, the liquid film is even forced to move counter-current. Therefore, the consequence of adopting a uniform velocity for the profile's injection is an over-injection of liquid and, as consequence, a lack in the injection of gas. If the counter-current liquid film scenario is considered, it would be necessary to remove liquid of the pipe during the injection of the measured signal, instead of adding it.

Besides the non-satisfactory result relating the Taylor-bubble length, the bubbles present in the flow act as Taylor bubbles, having their velocities close to that described by (Dumitrescu, 1943), since the beginning of the tube. The equivalence in the velocity becomes clear in Fig. 4, that compares the result of the two methods of fluid injection.

5. CONCLUSIONS

The modelling of a slug-flow inlet is a work in progress. There are different Boundary Conditions and simulations settings currently under study, but it can already be inferred that:

- A satisfactory slug flow was achieved using the numerical approach developed in this text.
- More improvements are required in order to achieve a functional injection of a measured slug flow pattern.

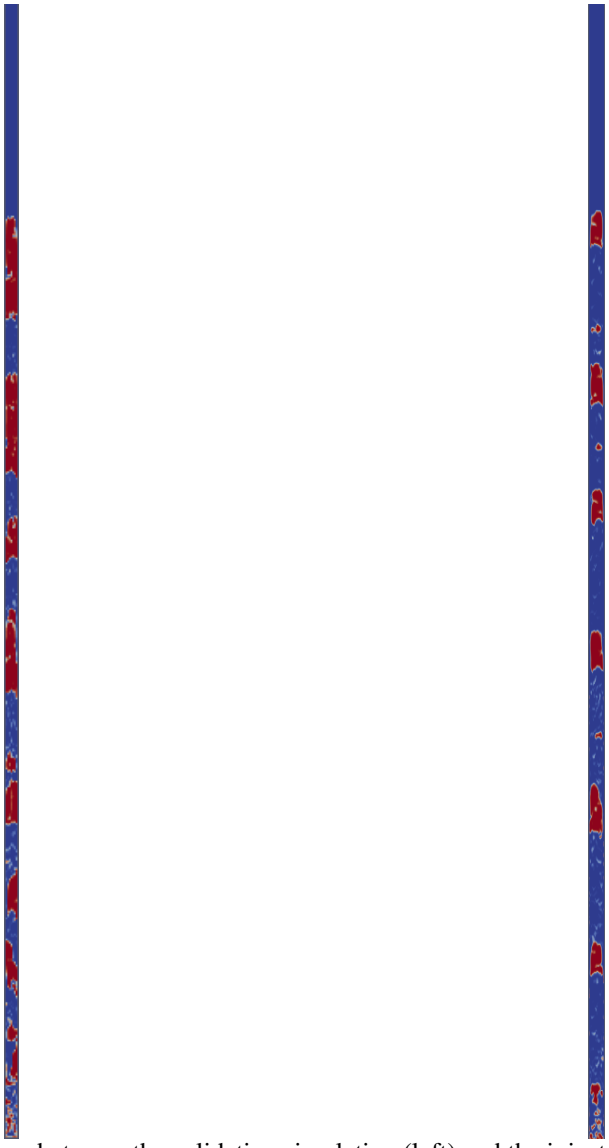

Figure 4: Comparison between the validation simulation (left) and the injected response (right).

- The PDF alone isn't sufficient to characterize the slug flow pattern, the velocity of the bubbles should also be considered.

- A slug-flow pattern was generated using the injection of fluids, but the length of the Taylor bubbles doesn't represent the original flow.

- The velocity distribution should also be considered during the injection of a developed slug flow pattern in the computational domain.

6. FUTURE PROJECTS

The method described in this text will be improved in the next months, and a satisfactory model response is expected before the conference. The final results will be presented in the conference poster.

7. ACKNOWLEDGEMENTS

the authors thank Petrobras and ANP ("Compromisso de Investimentos com Pesquisa e Desenvolvemento") for providing financial support for this work. Acknowledgments are also extended to ALFA - Artificial Lift & Flow Assurance Research Group.

8. REFERENCES

Abdulkadir, M., Hernandez-Perez, V., Lo, S., Lowndes, I. and Azzopardi, B.J., 2015. "Comparison of experimental and computational fluid dynamics (cfd) studies of slug flow in a vertical riser". *Experimental Thermal and Fluid Science*, Vol. 68, pp. 468–483.

Brackbill, J., Kothe, D.B. and Zemach, C., 1992. "A continuum method for modeling surface tension". *Journal of computational physics*, Vol. 100, No. 2, pp. 335–354.

Costigan, G. and Whalley, P., 1997. "Slug flow regime identification from dynamic void fraction measurements in vertical air-water flows". *International Journal of Multiphase Flow*, Vol. 23, No. 2, pp. 263 – 282. ISSN 0301-9322. doi:https://doi.org/10.1016/S0301-9322(96)00050-X. URL `http://www.sciencedirect.com/science/article/pii/S030193229600050X`.

Dumitrescu, D.T., 1943. "Strömung an einer luftblase im senkrechten rohr". *ZAMM-Journal of Applied Mathematics and Mechanics/Zeitschrift für Angewandte Mathematik und Mechanik*, Vol. 23, No. 3, pp. 139–149.

Hernandez-Perez, V., Abdulkadir, M. and Azzopardi, B., 2011. "Grid generation issues in the cfd modelling of two-phase flow in a pipe". *The Journal of Computational Multiphase Flows*, Vol. 3, No. 1, pp. 13–26.

Launder, B.E. and Spalding, D.B., 1983. "The numerical computation of turbulent flows". In *Numerical Prediction of Flow, Heat Transfer, Turbulence and Combustion*, Elsevier, pp. 96–116.

Schiller, L. and Naumann, Z., 1935. "A drag coefficient correllation". *Zeitschrift des Vereins Deutscher Ingenieure*, Vol. 77, p. 318.

Shuard, A.M., Mahmud, H.B. and King, A.J., 2016. "Comparison of two-phase pipe flow in openfoam with a mechanistic model". In *IOP Conference Series: Materials Science and Engineering*. IOP Publishing, Vol. 121, p. 012018.

Taitel, Y., Bornea, D. and Dukler, A., 1980. "Modelling flow pattern transitions for steady upward gas-liquid flow in vertical tubes". *AIChE Journal*, Vol. 26, No. 3, pp. 345–354.

Taitel, Y. and Dukler, A., 1976. "A model for predicting flow regime transitions in horizontal and near horizontal gas-liquid flow". *AIChE Journal*, Vol. 22, No. 1, pp. 47–55.

Tocci, F., 2016. *Assessment of a hybrid VOF two-fluid CFD solver for simulation of gas-liquid flows in vertical pipelines in OpenFOAM*. Master's thesis, Politecnico di Milano.

Wallis, G.B., 1969. *One-dimensional Two-phase Flow*. McGraw-Hill.

Wardle, K.E. and Weller, H.G., 2013. "Hybrid multiphase cfd solver for coupled dispersed/segregated flows in liquid-liquid extraction". *International Journal of Chemical Engineering*, Vol. 2013.

Weller, H.G., 2008. "A new approach to vof-based interface capturing methods for incompressible and compressible flow". *OpenCFD Ltd., Report TR/HGW*, Vol. 4.

9. RESPONSIBILITY NOTICE

The authors are the only responsible for the printed material included in this paper.